Dispatch-aware Planning of Energy Storage Systems in Active Distribution Network

Ji Hyun Yi, Rachid Cherkaoui, Mario Paolone
DESL, EPFL, Lausanne, Switzerland
{ji.yi, rachid.cherkaoui, mario.paolone}@epfl.ch

***Abstract*—This paper proposes a procedure for the optimal siting and sizing of energy storage systems (ESSs) within active distribution networks (ADNs) hosting a large amount of stochastic distributed renewable energy resources. The optimization objective is to minimize the ADN's day-ahead computed dispatch error. The allocation of ESS is determined while taking advantages from their operational features regarding the ADN's dispatchability. The proposed ESS planning is defined by formulating, and solving, a scenario-based non-linear non-convex optimal power flow (OPF). The OPF problem is converted to a piecewise linearized OPF (PWL-OPF). The ESS control strategy is designed to fully exploit the energy capacity of the ESS. It is integrated within the PWL-OPF to achieve the ADN's dispatchability regarding all operating scenarios. The Benders decomposition technique is employed to tackle the computational complexity of the proposed planning problem. The problem is decomposed into two sub-ones: a master problem where the allocation of the ESSs is decided, and several subproblems where the dispatchability of ADN with the support of the allocated ESS is evaluated through the scenario-based OPF. To validate the proposed method, extensive simulations are conducted on a real Swiss grid embedding significant PV generation capacity.**

***Index Terms*—Energy storage systems, optimal power flow, active distribution networks, resource planning, dispatchability**

NOMENCLATURE

Sets and Indices

$l, up(l) \in \mathcal{L}$	Index and set of nodes
$t \in \mathcal{T}$	Index and set of time steps
$\phi \in \Phi_d$	Index and set of scenarios for day d
$d \in \mathcal{D}$	Index and set of days
$m \in \mathcal{M}$	Index and set of benders iterations
υ	Index of discretization step for piecewise linearization

Variables

$U_l \in \{0,1\}$	Installation status of the ESS at node l
C_l	Energy reservoir of the ESS at node l
R_l	Power rating of the ESS at node l
$\tilde{p}_{lt}$	Average of the active load over all scenarios at node l for time t
$\Delta p_{l\phi t}$	Deviation of prosumption for scenario ϕ and time t from $\tilde{p}_{lt}$
$\tilde{f}_{lt}$	Average of squared current causing losses over all scenarios in line l for time t
$\Delta f_{l\phi t}$	Deviation of squared internal current for scenario ϕ and time t from the average $\tilde{f}_{lt}$
DP_t	Dispatch plan for time t at the grid connecting point (GCP)
F^E_{lt}	Offset profile for the ESS at node l, time t
$\omega_{l\phi t}$	Compensated error by the ESSs at node l, scenario ϕ, time t
$\epsilon_{l\phi t}$	Uncovered error at node l, scenario ϕ, time t
f_l	Squared current causing losses in line l
v_l	Squared voltage magnitude at node l
$s_l{=}p_l{+}jq_l$	Aggregated prosumption at node l
$S^t_l{=}P^t_l{+}jQ^t_l$	Upstream complex power flow to line l
$S^b_l{=}P^b_l{+}jQ^b_l$	Downstream complex power flow to node l from line l
$s^E_l{=}p^E_l{+}jq^E_l$	Complex power flow of ESS at node l
$E^E_{l\phi t}$	State-of-energy of ESS installed at node l for scenario ϕ and time t
μ_{ld}, ϑ_{ld}	Dual values at line l and day d for the ESS power rating and the energy reservoir

Parameters

Υ	Number of discretizations in the piecewise linear approximation function
θ^y_υ	of the υ-th slope in the disretization of y
$\bar{y}$	Maximum value of y.
b_l	Half of the total shunt susceptance of line l
$z_l = r_l{+}jx_l$	Total longitudinal impedance of line l
$\bar{I}_l$	Squared current upperbound of line l
$\bar{P}_l, \bar{Q}_l$	Maximum value of active and reacitve power flows for line l
$\bar{v}\backslash\underline{v}$	Upper bounds\Lower bounds of the squared nodal voltage magnitude
$\bar{E}_l\backslash\underline{E}_l$	Max.\min. *SoE* levels of ESS at node l
$\lambda_{\phi d}$	Probability of scenario ϕ on day d
α_d	Proxy subproblem costs for day d
$\bar{\mathcal{C}}_l\backslash\underline{\mathcal{C}}_l$	Max.\min. ESS energy reservoir at node l
$\bar{\mathcal{R}}_l\backslash\underline{\mathcal{R}}_l$	Max.\min. possible ESS power rating capacity at node l
$\underline{CR}$	Minimum power ramping rate of ESS
$\mathcal{I}_c, \mathcal{I}_e, \mathcal{I}_p$	ESS investment costs (fixed installation, energy reservoir, power rating)
w_l, w_f, w_e	Weight coefficients for the grid losses, offset profile, and dispatch error, respectively
N_d	Number of days in each day-type in a year
Y	ESS planning horizon

Submitted to the 21st Power Systems Computation Conference (PSCC 2020).

I. Introduction

The constant increase of spinning reserve in nowadays power systems is one of the technical concerns related to the increasing proportion of electricity production from distributed stochastic resources. [1] The security of the power system has been traditionally sustained by central procurement of regulating power from fast generating units. However, the growing uncertainty associated to power generation of stochastic resources calls for higher expenses for the procurement of conventional reserve. In this respect, the recent literature has advocated the provision of flexibility from active distribution networks (ADNs) such as demand-side management and energy storage systems (ESSs) [2]. In particular, there has been increasing interest in using ESSs in ADNs to compensate for the uncertainty of non-dispatchable local resources (e.g., [3], [4]). Efforts have been made to achieve *dispatchability* of the ADNs in view of the inherent advantages such as reduction of the bulk system reserve provision [1] and mitigation of the imbalance penalty charges imposed on distribution system operators (DSOs) [5], [6].

The *dispatchability* signifies the capability of the ADN active power flow through the grid connecting point (GCP) with the transmission netowrk to strictly follow a day-ahead power schedule composed of discrete intervals, henceforth called *dispatch plan*. Due to the inherent stochasticity of prosumption[1], the realized active power infeed at the GCP varies from the dispatch plan. The magnitude of the difference is defined as *dispatch error*. When ESSs are exploited to compensate the dispatch error, a DSO of an ADN can have a sufficient capability to control the network infeed through the GCP close to the dispatch plan, thereby avoiding high penalties for power imbalance [7]. Based on the probabilistic forecast of the prosumption and forecast errors, the Authors of [5] compute an optimal dispatch schedule by minimizing the power exchange through the GCP, while limiting the occurrences of dispatch error during the total operation horizon. Meanwhile, a robust optimization approach with an emphasis on control strategy for ESS is proposed in [6]. The Authors suggest an operational procedure to obtain a dispatch plan taking into account the ESS control strategy that can maximize the ESS exploitation to cope with the prosumption forecasting uncertainty. However, the algorithm proposed in [5], [6] do not take into account the network model and associated operational constraints, which may lead to solutions that are physically inapplicable during the real operation. The operational constraints were addressed to compute an optimal dispatch plan in [8], but the model did not involve any control strategy of ESS. In [9], the Authors presented a control-aware optimal placement and sizing of ESSs by embedding receding horizon control strategies within a linearized optimal power flow (OPF). However, the objective of the problem was to maximize the photovoltaic utilization, rather than achieving the dispatchability of the targeted grid.

[1] *Prosumption* is defined as the load consumption minus the generated power from local generation.

Notably, the above mentioned studies clearly state that the feasibility of the formulated problems regarding the imbalance constraint is heavily dependent on the ESS capacity. There has been papers in probabilistic estimation of the required ESS capacity to compensate the renewable generation uncertainty to pre-defined extent from the prosumer's side [10], [11]. However, regarding the purpose of achieving the dispatchability of the ADN, it is necessary to evaluate the optimal allocation of ESS in the view of DSOs' economic profit by considering the trade-off between its investment cost and the expected advantages, while respecting the technical requirements for the preferred operational condition of the ADN.

Based on this fundamental observation, the Authors of this paper proposed an OPF-based ESS planning strategy to achieve the dispatchability of ADNs in [12]. The objective of the ADN is defined as to minimize the dispatch error during the ADN operation horizon. The optimization problem regarding the ESS allocation consists of a two-stage decision process. The first-stage decision is associated with the investment of ESS which is determined by the location and the capacity of the ESSs energy reservoirs and power ratings. The second-stage decision is related to the daily operation of ADN with allocated ESSs concerning several operating scenarios.

Meanwhile, the control strategy of ESS can profoundly influence the ESS allocation by providing an efficient way to use their capacity for handling the local resources' uncertainties [13]. Therefore, it is worth exploring the impact of the control aspect of ESSs while optimizing their capacity. However, to the best of the Authors' knowledge, the previous literature has not focused on this specific problem. In this respect, this paper is an extension of [12] with an emphasis on the integration of ESS control scheme within the planning problem.

The operation of ESS must adhere to the chosen control strategy while ensuring operational conditions of the ADN to be technically feasible. Therefore, the performance and reliability of the planning tools for ADNs can be guaranteed only when the operational conditions of the system are accurately modeled through a proper OPF model. Among various approaches, we focus on convex AC-OPF models in view of their superiority in guaranteeing the optimality of the solution. One of the consolidated approaches for the convexification of the AC-OPF is provided by relaxation methods, such as semi-definite programming (SDP) [14] or second-order cone programing (SOCP) proposed for radial grids [15]. The SOCP relaxation is preferred in several studies for solving the ESS sizing problem thanks to its computational efficiency and tractability [16], [17]. The author of [18] pointed out the drawbacks of the SOCP relaxation method such as the possible inexactness of the solution in the cases of reverse line power flows and the cases where the upper bound of nodal voltage and line ampacity constraints are binding. Then, the authors proposed the so-called Augmented Relaxed OPF (AR-OPF), which is capable to guarantee the exactness of the solution by constructing an augmented conservative set of constraints. In [12], the AR-OPF model has been leveraged for solving the optimization problem of the ESS allocation by achieving

the ADN dispatchability. The objective function for the given problem has been deliberately modified to comply with a prerequisite condition of the AR-OPF objective function in order to guarantee the exactness of the solution. The condition states the objective function should strictly increase with the grid losses.

In this paper, embedding the ESS control strategy requires the optimization problem to have more flexibility with repsect to the objective function. It should be noted that integrating the control scheme within the AR-OPF problem might violate the prerequisite condition on the objective function for the exactness of the solution. In this regard, we choose to utilize an alternative convexification approach through linear approximation of the original power flow equations. The linear approximated model makes the OPF problem more tractable at the expense of the exactness of the formulation (i.e., the optimal solution of the approximated model may not be equivalent to the optimal solution of the original OPF problem). The first approach employs the linear approximation of nodal voltages and current flows as function of nodal power injections [19], [20]. Another approach relies on approximating the nonlinear terms in the power flow equations, such as piecewise linearized OPF (PWL-OPF). The piecewise linearization method is widely used in tackling various research interests in power system thanks to its flexibility of implementation [21]–[23]. It can achieve the optimal solution of reasonable quality, with minor approximation error from the original OPF solution.

In this context, PWL method is employed for the ESS control-aware planning problem. Moreover, it is noteworthy that the proposed planning strategy can be applicable not only in radial grids but also in meshed grids by using PWL-OPF model. Unlike the existing work relying on the PWL method, we take into account the shunt element of the lines in the PWL-OPF model, which can bring a significant impact on line current especially in the networks with underground coaxial cables. Moreover, we embed the operational strategy for ESS to utilize its energy capacity optimally to cope with uncertainty in the power flow through the distribution feeder. The planning problem is formulated as a mixed-integer linear programming (MILP) problem, which is notorious for its computational intractability. In this respect, the Benders decomposition is employed [24]. The contributions of the paper are listed below.

1) The optimal allocation of ESSs is determined based on an piecewise linear approximation of the full AC-OPF to achieve the dispatchability of an ADN hosting a high capacity of stochastic renewable generation.
2) The control-aware approach embeds the maximum exploitation of ESSs capacity, and is integrated into the ESSs planning problem.

The structure of the paper is as follows: in Section II, we describe the proposed method and the differences with respect to our former work [12]. In Section III, the proposed problem formulation and solution approach are described, followed by a specific case study illustrated in Section IV. Finally, Section V concludes the paper.

II. The Method

In this section, the main characteristics of the proposed method are described. The formulation of the operational strategy to achieve dispatchability of ADN is recalled and then followed by the description of the modified PWL-OPF model.

A. Key differences with AR-OPF planning approach [12]

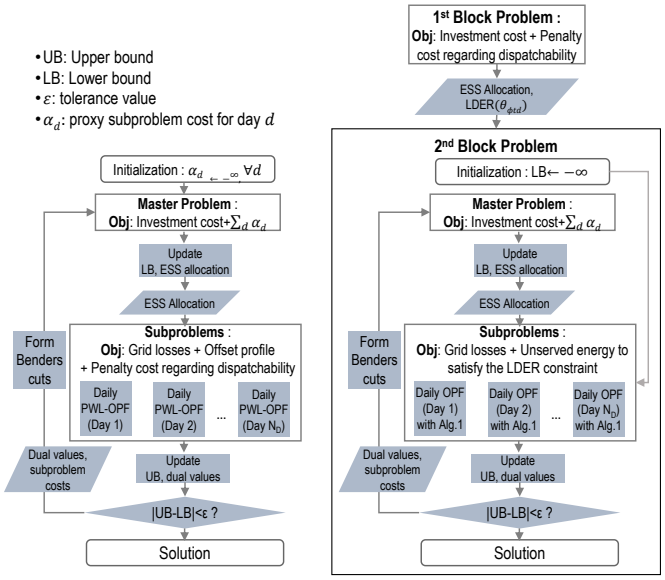

(a) (b)

Fig. 1. The full algorithm: (a) This paper, (b) [12].

In spite of the shared objective and the similar decision making stages, [12] and this paper have significant differences in the solution approach for the OPF problem and the overall structure of the problem formulation.

The righthand side of Fig. 1 depicts the full algorithm for the ESSs planning scheme presented in [12]. In [12], the primary interest lies in obtaining an exact optimal solution regarding the operating points for the considered operation horizon. Therefore, the construction of the problem is centered around the compliance with the condition for guaranteeing the exactness of the optimal solution of the AR-OPF model, which requires the objective function to be strictly increasing with the total grid losses. However, the dispatch error[2] does not increase while the total grid losses increase.

In this regard, we separately treated the objective of minimizing the dispatch error apart from the AR-OPF problem by introducing it into the objective function of the first block problem. It solves the optimal planning problem of ESS with a simplified linear OPF neglecting the line losses. The role of the 1st block is to yield the optimal leftover dispatch error rate (LDER) considering both the ESSs investment cost and their operational benefit. The LDER then serves as an operational constraint for the OPF problem formulated with the non-approximated, but convex, AR-OPF model in

[2]The associated mathematical formulation is further discussed in Sec. II-B.

the second block. The second block is decomposed into a master problem and several parallel subproblems. The master problem seeks for the optimal allocation taking into account the subproblem costs, which evaluate the suffciency of the ESS capacity to comply with the dispatch LDER constraint over all prosumption scenarios. Through the Benders decomposition, the allocation of ESS is determined such that the dispatch LDER constraint can be satisfied without any load curtailment. It is worthwhile to know that the OPF problem defined in each subproblem lacks the inclusion of ESS control strategy.

In this paper, we put our attention primarily on maximizing the controllability of the allocated ESS asset by implementing the control strategy of ESSs within the OPF problem. In this respect, the PWL-OPF model is selected to approximate the full AC-OPF. It enables enhancing the flexibility regarding the choice of objective by relaxing the exactness of the solution, so that the control strategy for ESS can be added to the objective function of the PWL-OPF problem along with the objective term regarding the minimization of dispatch error. Unlike in [12], the decision process of the ESS allocation can start directly with the initial stage of the Benders decomposition (see the lefthand side of Fig. 1). As the Benders iteration progresses, the optimal LDER is determined within the sub-problems in terms of the operational benefit brought by the ESS allocation.

B. Construction of the dispatch plan

As described in (1) and (2), the active prosumption and the grid losses are respectively expressed by two components: prediction, and deviation from the prediction point (we would define it as *error* hereafter). The total error of prosumption and line losses over all nodes and lines is equivalent to dispatch error. It can be compensated by the installed ESSs as much as their capacity allows. In order to quantify the error covered and not covered by the ESSs, we express the dispatch error as (3). $\omega_{l\phi t}$ and $\epsilon_{l\phi t}$ represent the error covered by ESS and the leftover error that cannot be covered at each node l with respect to scenario ϕ and time t, respectively. The sum of leftover error over all nodes corresponds to the uncovered dispatch error in each operating scenario.

$$\tilde{p}_{lt} = p_{l\phi t} + \Delta p_{l\phi t},\ \forall l \in \mathcal{L}, \forall \phi \in \Phi_d, \forall t \in \mathcal{T} \tag{1}$$

$$r_l \tilde{f}_{lt} = r_l f_{l\phi t} + r_l \Delta f_{l\phi t},\ \forall l \in \mathcal{L}, \forall \phi \in \Phi_d, \forall t \in \mathcal{T} \tag{2}$$

$$\sum_{l\in\mathcal{L}} (\Delta p_{l\phi t} + r_l \Delta f_{l\phi t}) = \sum_{l\in\mathcal{L}} (\epsilon_{l\phi t} + \omega_{l\phi t}),\ \forall \phi \in \Phi_d, \forall t \in \mathcal{T} \tag{3}$$

The daily dispatch plan is determined by the predicted point of the total prosumption considering the grid losses. The prediction profile of prosumption is calculated by averaging the scenario profiles [6], considering that the prosumption scenarios for each day are generated assuming the prosumption profile follows a normal probability distribution. More importantly, the daily dispatch plan also includes ESSs control term, namely the so-called *offset profile*, to maximize the exploitation of the ESSs capacity to cover the uncertainty of the prosumption [6]. The objective of the offset profile is to restore an adequate ESSs state-of-energy (SoE) so that enough flexibility is available within ESSs to compensate upcoming error between the predicted and the realized prosumption during operation. For example, assume that the current SoE of the ESS is near SoE limit, and the high uncertainty (i.e. the realized prosumption deviates from the forecasted prosumption with large magnitude.) is expected in upcoming time intervals. Then, the offset profile assigned to each allocated ESS takes value to bias the dispatch plan to charge/discharge to/from the ESS, such that the SoE level of the ESS is adjusted to a state capable to compensate for the largest realizations of prosumption forecast errors. It makes the ESS have a high capability of compensating for the uncertainty projected up to the end of the dispatch horizon.

(4) indicates that the offset profile F^E_{lt} is assigned to the ESS allocated at node l, where Z stands for a big number. The ESS active power dispatch at node l is determined at every time interval t with the offset profile and the power compensating the dispatch error, as shown in (5).

$$|F^E_{lt}| \leq Z * U_l,\ \forall l \in \mathcal{L}, \forall t \in \mathcal{T} \tag{4}$$

$$p^E_{l\phi t} = F^E_{lt} + \omega_{l\phi t},\ \forall l \in \mathcal{L}, \forall \phi \in \Phi_d, \forall t \in \mathcal{T} \tag{5}$$

Each offset profile assigned to an ESS is added into the dispatch plan. In this way, the energy required to restore the appropriate SoE can be embedded in the dispatch plan. The dispatch plan for an ADN considering grid losses is finally expressed as (6) by incorporting (1) and (2), along with the offest profiles.

$$DP_t = \sum_{l\in\mathcal{L}} F^E_{lt} + \sum_{l\in\mathcal{L}} (\tilde{p}_{lt} + r_l \tilde{f}_{lt}),\ \forall t \in \mathcal{T} \tag{6}$$

Finally, achieving the dispatchability during the operation horizon can be mathematically expressed by minimizing the sum of the absolute value of the uncovered dispatch error for all the considered prosumption scenarios in set Φ_d during the dispatch horizon $\mathcal{T}$. On top of that, in order to leverage the ESSs control strategy, the sum of the absolute value of the offset profiles associated to ESSs over all time intervals is embedded for the minimization problem. In this way, the dispatch plan is optimally determined such that the dispatch error is minimized with the maximum exploitation of ESS controlled by the offset profile.

C. Piecewise Linear Optimal Power Flow

The operational benefit of ESS allocation for the ADN is evaluated through solving daily OPF problems. The OPF formulation for a radial power network is derived by applying the Kirchhoff's law to Fig. 2, which depicts the line model for a radial power network. The power flow equations are given in (7a)-(7d). $\mathbf{G}$ is the adjacency matrix of the network, where $\mathbf{G}_{k,l}$ is defined for $k, l \in \mathcal{L}$ and $\mathbf{G}_{k,l} = 1$ if $k = up(l)$ or 0 if not. The grid security constraints regarding nodal voltages and the line ampacity are expressed with (7e) and (7f), (7g) respectively.

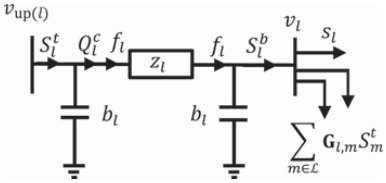

Fig. 2. Classic two-port Π model of a transmission line adopted for the formulation of the OPF relaxed constratins [18].

$$S_l^t = s_l + \sum_{m\in\mathcal{L}} \mathbf{G}_{l,m}\, S_l^t + z_l\, f_l - (v_{up(l)} + v_l) b_l,\ \forall l \in \mathcal{L} \tag{7a}$$

$$S_l^b = s_l + \sum_{m\in\mathcal{L}} \mathbf{G}_{l,m}\, S_l^t,\ \forall l \in \mathcal{L} \tag{7b}$$

$$v_l = v_{up(l)} - 2\Re\left(z_l^* \left(S_l^t + j v_{up(l)} b_l \right) \right) + |z_l|^2\, f_l,\ \forall l \in \mathcal{L} \tag{7c}$$

$$f_l = \frac{|P_l^t|^2 + |Q_l^t + v_{up(l)} b_l|^2}{v_{up(l)}} = \frac{|P_l^b|^2 + |Q_l^b - v_l b_l|^2}{v_l},\ \forall l \in \mathcal{L} \tag{7d}$$

$$\underline{v}_l \le v_l \le \bar{v}_l \tag{7e}$$

$$\frac{|P_l^t|^2 + |Q_l^t|^2}{v_{up(l)}} \le \bar{I}_l, \forall l \in \mathcal{L} \tag{7f}$$

$$\frac{|P_l^b|^2 + |Q_l^b|^2}{v_{(l)}} \le \bar{I}_l, \forall l \in \mathcal{L} \tag{7g}$$

(7d), (7f), and (7g) contain quadratic terms and fraction terms which make them non-convex, and thus computationally burdensome. Therefore, we apply a piecewise linearization and simplification on the non-linear terms. The first stage is to slimplify the fraction term by replacing the denominator variables associated with the nodal voltage magnitude in (7d), (7f), and (7g) with the voltage lowerbound ($\underline{v}_l$). This results in upper approximation on the line current and the current causing the grid losses. In this way, the simplification ensures the feasible operation of ADN over the operating scenarios by building conservative constraint on the line ampacity. Taking only the first part of (7d), the equation is simplified to (8a). (7f) and (7g) is replaced with (8b) and (8c).

$$\underline{v}_l f_l = |P_l^t|^2 + |Q_l^t + v_{up(l)} b_l|^2,\ \forall l \in \mathcal{L} \tag{8a}$$

$$|P_l^t|^2 + |Q_l^t|^2 \le \underline{v}_l \bar{I}_l, \forall l \in \mathcal{L} \tag{8b}$$

$$|P_l^b|^2 + |Q_l^b|^2 \le \underline{v}_l \bar{I}_l, \forall l \in \mathcal{L} \tag{8c}$$

Then, we linearize (8a)-(8c) by applying the PWL method on the quadratic terms: $|P_l^t|^2, |P_l^b|^2, |Q_l^t|^2, |Q_l^b|^2$, and $|Q_l^t + v_{up(l)} b_l|^2$, by utilizing a piecewise linear approximation function [21] formulated by the equations below.

$$|P_l^t|^2 \approx f(P_l^t, \bar{P}_l, \Upsilon) \quad \forall l \in \mathcal{L} \tag{9a}$$

$$|Q_l^t|^2 \approx f(Q_l^t, \bar{Q}_l, \Upsilon) \quad \forall l \in \mathcal{L} \tag{9b}$$

$$|P_l^b|^2 \approx f(P_l^b, \bar{P}_l, \Upsilon) \quad \forall l \in \mathcal{L} \tag{9c}$$

$$|Q_l^b|^2 \approx f(Q_l^b, \bar{Q}_l, \Upsilon) \quad \forall l \in \mathcal{L} \tag{9d}$$

$$|Q_l^t + v_{up(l)} b_l|^2 \approx f(Q_l^t + v_{up(l)} b_l, \bar{Q}_l, \Upsilon) \quad \forall l \in \mathcal{L} \tag{9e}$$

where $\bar{P}_l$ and $\bar{Q}_l$ are chosen as the maximum active power flow and reactive power flow over all scenarios and timesteps for each line, which are obtained by running a preliminary load flow with the selected stochastic prosumption scenarios. The piecewise linear approximation function $f(y, \bar{y}, \Upsilon)$ approximates the quadratic curve of y as shown in (10a).

$$f(y, \bar{y}, \Upsilon) = \sum_{\upsilon=1}^{\Upsilon} \theta_\upsilon^y \Delta_\upsilon^y \tag{10a}$$

$$y = y^+ - y^-, \quad y^+, y^- \in \mathbb{R}^+ \tag{10b}$$

$$y^+ + y^- = \sum_{\upsilon=1}^{\Upsilon} \Delta_\upsilon^y \tag{10c}$$

$$0 \le \Delta_\upsilon^y \le \bar{y}/\Upsilon \quad \forall \upsilon = 1, ..., \Upsilon \tag{10d}$$

$$\theta_\upsilon^y = (2\upsilon - 1)\bar{y}/\Upsilon \quad \forall \upsilon = 1, ..., \Upsilon \tag{10e}$$

(10b) says that y is expressed by subtracting two non-negative variables y^+ and y^-, which represent the positive value of y and the negative value of y, respectively. In this way, the absolue value of y can be expressed by the two variables as shown in the left-hand side of (10c). An auxilary variable Δ_υ^y is introduced to determine the step size for the piecewise discretization of the aboslute value of y. Each step size is optimally decided within the range specified in (10d), which is governed by the number of discretized segments and $\bar{y}$ which stands for the maximum value of y. With each discretization step, θ_υ^y, which is the slope of each discretized line, is determined by (10e) is assigned to construct the set of line segments, which all together approximate the quadratic value of y (see (10a)).

By using the piecewise linear approximation function, all the quadratic terms indicated in the OPF formulation can be replaced. Therefore, (8a) can be replaced with (11a), and (8b), (8c) with (11b) and (11c).

$$\underline{v}_l f_l = f(P_l^t, \bar{P}_l, \Upsilon) + f(Q_l^t + v_{up(l)} b_l, \bar{Q}_l, \Upsilon),\ \forall l \in \mathcal{L} \tag{11a}$$

$$f(P_l^t, \bar{P}_l, \Upsilon) + f(Q_l^t, \bar{Q}_l, \Upsilon) \le \underline{v}_l \bar{I}_l,\ \forall l \in \mathcal{L} \tag{11b}$$

$$f(P_l^b, \bar{P}_l, \Upsilon) + f(Q_l^b, \bar{Q}_l, \Upsilon) \le \underline{v}_l \bar{I}_l,\ \forall l \in \mathcal{L} \tag{11c}$$

In this paper, we chose $\Upsilon = 30$, and the corresponding approximation error is evaluated by calculating the difference in the longitudinal line current causing losses between the approximated value ($\sqrt{f_l}$) and actual value ($\sqrt{\frac{|P_l^t|^2 + |Q_l^t + v_{up(l)} b_l|^2}{v_{up(l)}}}$). The mean value was 4.85e-4 p.u. and the maximum value was 4.2e-3 p.u. where the base current value is 165 A.

For the sake of keeping the paper readable, the power flow equations (7a)-(7c), (11a), and security constraints (7e), (11b) and (11c) employing the PWL method are grouped and synthetically expressed as $\Theta(\varphi, \kappa) \ge 0, \forall l \in \mathcal{L}$ where $\varphi = \{\Delta_\upsilon^{P_l^t}, \Delta_\upsilon^{Q_l^t}, \Delta_\upsilon^{P_l^b}, \Delta_\upsilon^{Q_l^b}, \Delta_\upsilon^{Q_l^t + v_{up(l)} b_l}, S_l^t, v_l, f_l, s_l\}$ is the set of variables and the set of parameters is given as $\kappa = \{z_l, b_l, \bar{v}_l, \underline{v}_l, \bar{I}_l, \theta_\upsilon^{P_l^t}, \theta_\upsilon^{Q_l^t}, \theta_\upsilon^{P_l^b}, \theta_\upsilon^{Q_l^b}, \theta_\upsilon^{Q_l^t + v_{up(l)} b_l}, \Upsilon\}$.

III. Problem Formulation

The objective of the problem is to determine the optimal sizes and sites of ESSs so that the power flow through the ADN GCP follows a daily dispatch plan with a minimal deviation. As previously mentioned, by embedding the offset profile within the dispatch plan, we can maximize the exploitation of the installed ESSs to cope with the uncertainty caused by stochastic nature of the resources. The problem is formulated as a two-stage stochastic MILP model. The first stage is associated with the ESS investment. With the allocation of ESS fixed by the solution obtained from the first stage, the second stage minimizes the expected penalty cost on the uncovered dispatch error with respect to the operating scenarios for during the daily operation. For the computational efficiency, we select a number of typical days that can reflect the seasonal variation of the prosumption over a year.

To tackle the complexity of the problem, the Benders decomposition technique is employed to decompose the problem into two problems: the master problem which determines the sites and sizes of the ESSs, and the several subproblems that each represent the daily operation for different day types where the fitness of the determined allocations is evaluated with respect to the grid losses and the dispatch error. The whole stucture is illustrated in the lefthand side of Fig. 1. The Benders decomposition algorithm starts with the evaluation of the operational condition of ADN in a default configuration. The evaluation is fed back into the master problem to re-decide on the optimal ESS allocation in the view of improvement on the operational condition. The decomposition procedure goes through a number of iterations between solving the master problem and several subproblems until it reaches a convergence.

A. Master problem

In the master problem, the optimal siting and sizing of the ESSs is determined considering the investment cost and the proxy subproblem costs. The formulation of the master problem is given in (12a), minimizing the total planning cost computed by adding the investment cost, which consists of fixed installation costs, power rating costs, and energy reservoir costs, with the sum of lower approximations for the subproblem costs with respect to the determined ESSs allocation. The optimization variables of the problem are given in (12g) and the constraints are given as (12b)-(12f).

$$\min_{\Omega_1} \sum_{l\in\mathcal{L}} (\mathcal{I}_c U_l + \mathcal{I}_p R_l + \mathcal{I}_e C_l) + \sum_{d\in\mathcal{D}} \alpha_d \tag{12a}$$

Subject to:

$$\underline{\mathcal{R}}_l U_l \le R_l \le \bar{\mathcal{R}}_l U_l,\ \forall l \in \mathcal{L}, \tag{12b}$$

$$\underline{\mathcal{C}}_l U_l \le C_l \le \bar{\mathcal{C}}_l U_l,\ \forall l \in \mathcal{L}, \tag{12c}$$

$$R_l \le \frac{C_l}{\underline{CR}},\ \forall l \in \mathcal{L}, \tag{12d}$$

$$\alpha_d \ge \underline{\alpha},\ \forall d \in \mathcal{D}, \tag{12e}$$

$$\alpha_d \ge \Gamma_d^{(m)},\ \forall d \in \mathcal{D}, \forall m \in \mathcal{M}. \tag{12f}$$

$$\Omega_1 = \{U_l, C_l, R_l, \alpha_d\},\ \forall l \in \mathcal{L}, \forall d \in \mathcal{D} \tag{12g}$$

$$LB = \sum_{l\in\mathcal{L}} (\mathcal{I}_c U_l^* + \mathcal{I}_p R_l^* + \mathcal{I}_e C_l^*) + \sum_{d\in\mathcal{D}} \alpha_d^* \tag{13}$$

The constraints related to the ESS allocation are given as (12b)-(12d). Possible energy reservoir and power rating capacities are limited due to manufacturing and geographical restrictions, as described in (12b) and (12c). Typically, the maximum power discharged from an ESS is governed by the maximum capacity with a certain rate (such as C-rate for batteries) (see (12d)). In the initial stage of Benders decomposition, the approximated cost of the subproblem associated with day d, or α_d, is assigned with the pre-defined lower bound for the subproblem cost $\underline{\alpha}$. As the decomposition procedure progresses, it improves the approximation by the set of Benders cuts ($\Gamma_d^{(m)}, \forall d, \forall m \in \mathcal{M}$), which is added at every benders iteration as shown in (12f) (see (18)). After solving the master problem, the lower bound for the total planning cost, or LB, is updated with the optimal objective value as shown in (13) (* indicates that it is the identified optimal solution).

B. Subproblem

In the subproblem associated with day d, a daily PWL-OPF model evaluates the operational benefits of ESSs with respect to the dispatchability and losses minimization under the compliance with the grid constraints. The dispatch plan embedding the offset profile is computed to follow the prosumption scenarios. Meanwhile, the dispatchability of CGP with respect to the dispatch plan is evaluated in terms of uncovered dispatch error while maximizing the exploitation of the determined ESS for compensation of the dispatch error.

1) Modeling of ESSs operation: The operational characteristics of an ideal ESS are modeled to reflect the behavior of the allocated ESSs during the daily operation of ADN. The active and reactive power outputs of the ESS are governed by the capability curve defined by the maximum apparent power of the ESS. We linearize the associated circular capability curve by constructing an inscribed square within the original curve (see (14a)). (14b) describes the dynamic behavior of SoE level of each ESS depending on the charge/discharge power flows at every time interval. Δt stands for the time resolution. (14c) indicates that the SoE level of the ESS should be within the upper and lower SoE limits.

$$-\frac{R_l}{\sqrt{2}} \le p_{l\phi t}^E \le \frac{R_l}{\sqrt{2}}, \quad -\frac{R_l}{\sqrt{2}} \le q_{l\phi t}^E \le \frac{R_l}{\sqrt{2}}, \quad \forall l \in \mathcal{L}, \forall \phi \in \Phi_d, \forall t \in \mathcal{T} \tag{14a}$$

$$E_{l\phi(t+1)}^E = E_{l\phi t}^E + \Delta t * p_{l\phi t}^E,\ \forall l \in \mathcal{L}, \forall \phi \in \Phi_d, \forall t \in \mathcal{T} \tag{14b}$$

$$\underline{E}_l C_l \le E_{l\phi t}^E \le \bar{E}_l C_l,\ \forall l \in \mathcal{L}, \forall \phi \in \Phi_d, \forall t \in \mathcal{T} \tag{14c}$$

To consider the ESS for the daily operation of ADN, the model of ESS operation should be included in the set of power flow equations defined for all scenarios and time intervals within the daily dispatch horizon. Henceforth, the equations of the PWL-OPF model, including the ESSs are re-defined as:

$$\Theta(\varphi'_{\phi t}, \kappa) \ge 0,\ \forall l \in \mathcal{L}, \forall \phi \in \Phi_d, \forall t \in \mathcal{T}, \tag{15}$$

where $\varphi'_{\phi t}=\{\Delta_v^{P^t_{l\phi t}}, \Delta_v^{Q^t_{l\phi t}}, \Delta_v^{P^b_{l\phi t}}, \Delta_v^{Q^b_{l\phi t}}, \Delta_v^{Q^t_{l\phi t}+v_{up(l)\phi t}b_l}, S^t_{l\phi t}, v_{l\phi t}, f_{l\phi t}, s_{l\phi t}=(p_{l\phi t}+p^E_{l\phi t})+j(q_{l\phi t}+q^E_{l\phi t})\}$ is the set of variables and $\kappa=\{z_l, b_l, \bar{v}_l, \underline{v}_l, \bar{I}_l, \theta_v^{P^t_l}, \theta_v^{Q^t_l}, \theta_v^{P^b_l}, \theta_v^{Q^b_l}, \theta_v^{Q^t_l+v_{up(l)}b_l}, \Upsilon\}$ is the set of parameters.

2) Mathematical formulation: As indicated in (16a), the objective of the subproblem is to minimize the uncovered dispatch error, the absolute value of the offset profile, and the grid losses, with the set of optimization variables defined as (16d). The constraints include power flow equations and security constraints (see (15)) along with the set of equations associated with achieving dispatchability (see (1)-(6)) described in Sec. II-B. Moreover, the constraints (16b) and (16c) describe that the ESS power ratings and the energy reservoirs are fixed to the optimal solution of the master problem.

$$\min_{\Omega_2} : \mathcal{SC}_d = YN_d \sum_{t\in\mathcal{T}}(w_f \sum_{l\in\mathcal{L}} |F^E_{lt}| + \sum_{\phi\in\Phi_d} \lambda_{\phi d}(w_e|\sum_{l\in\mathcal{L}} \epsilon_{l\phi t}| + w_l \sum_{l\in\mathcal{L}} r_l f_{l\phi t})) \tag{16a}$$

Subject to:
(1)-(6), (14), (15),

$$R_l = R^*_l : \mu_{ld},\ \forall l \in \mathcal{L}, \tag{16b}$$

$$C_l = C^*_l : \vartheta_{ld},\ \forall l \in \mathcal{L}. \tag{16c}$$

$$\Omega_2 = \{\varphi'_{\phi,t}, F^E_{lt}, \omega_{l\phi t}, E_{l\phi t}, C_l, R_l\},\ \forall l \in \mathcal{L}, \forall \phi \in \Phi_d, \forall t \in \mathcal{T} \tag{16d}$$

where w_f, w_e and w_l are the weight coefficients for the offset profile, dispatch error, and grid losses, respectively. μ_{ld} and ϑ_{ld} are the dual of constraints related to the fixed ESS capacities. $m \in \mathcal{M}$ is the index of benders iterations. The dual values obtained in mth iteration are provided as inputs to the master problem in next iteration to form Benders cuts (see (18)). The upper bound of the total planning cost UB is calculated by adding the optimal investment cost obtained from the master problem and the sum of parallel subproblem costs over all days as shown in (17).

$$UB = \sum_{l\in\mathcal{L}}(\mathcal{I}_c U^*_l + \mathcal{I}_p R^*_l + \mathcal{I}_e C^*_l) + \sum_{d\in\mathcal{D}} \mathcal{SC}^*_d \tag{17}$$

$$\Gamma^{(m)}_d = \big[\mathcal{SC}^*_d - \sum_{l\in\mathcal{L}}(\mu_{ld}(R_l - R^*_l) - \vartheta_{ld}(C_l - C^*_l))\big], \quad \forall d \in \mathcal{D}, \forall m \in \mathcal{M} \tag{18}$$

IV. Case Study

A. Simulation configuration

In this section, the proposed method is tested with an existing Swiss distribution network hosting a large capacity of renewable generation (see Fig. 3). The base voltage is 21kV, and the base 3 phase power is 6MVA. The total capacity of the PV generation is 2.7MWp, whereas the total capacity of hydropower generation is 805kVA. The planning horizon is set as 10 years. All the parameters related to the investment of ESS are listed in Table I. The stochastic nature of load consumption and PV injections is considered by generating operating scenarios based on the historical data provided by the local DSO.[3] In order to mitigate the computational burden, we assume that the seasonal variation of the prosumption over the year can be represented with 8 typical days. All the days are independent and thus not linked to each other. For each day type, the uncertainty of the forecast is modeled by generating 1000 prosumption scenarios, which are reduced to 10 scenarios based on K-medoids clustering algorithm [25]. The dispatch time interval for a daily operation is set as 15 min. The penalty cost for the dispatch error is set as \$700/MWh. It is worth observing that this price is intentionally set to be substantially higher than the typical imbalance cost observed in power energy markets [26] to put a high priority on achieving dispatchability of the distribution grid.

TABLE I
ESS Parameter and Candidate Nodes for Simulation

Maximum power rating per site	3MW	Maximum energy reservoir per site	4MWh
Installation cost for energy reservoir	\$300/kWh	Installation cost for power rating	\$200/kVA
Capital investment cost per site		\$0.1Million	
Candidate nodes for ESS		4, 16, 27, 41, 45	

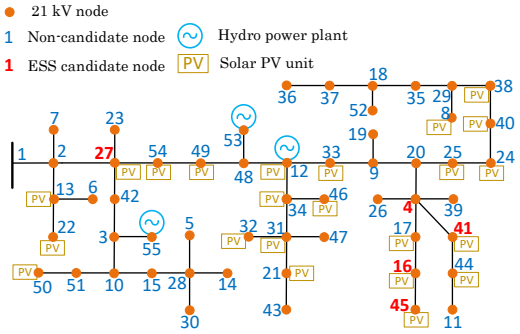

Fig. 3. Considered real 55 node distribution feeder.

B. Simulation Result

To verify the effectiveness of the ESS control scheme, we demonstrate the simulation results considering two cases that differ in control approaches: case 1 with the offset profile embedded into a dispatch plan and case 2 without it. The optimal siting and sizing of ESSs are shown in Table II followed by Table III, where the operational advantages of the ESS allocation are indicated in terms of penalty cost for the dispatch error and grid losses. At Node 4, both of the ESS energy reservoirs and power ratings are bigger in case 1 than in case 2, whereas at Node 27, the ESS energy reservoir is bigger in case 1 but the power ratings are similar in both cases (see Table II). The overall investment cost is \$0.15 Million larger in case 1, and the annual uncovered dispatch error is 51.77 MWh lower in case 1 (see Table III), leading to reduction of \$0.2

[3]Since the proposed method relies on a scenario-based approach, the modeler can use generic parametric and non-parametric distributions to model the prosumptions. In this paper, the active and reactive prosumption scenarios for each day are generated assuming the prosumption profile follows a normal distribution.

Million in the total cost. This difference in allocation and the dispatch result can be associated with the efficiency of the ESS control scheme. Thanks to the offset profile, the utilization of the energy reservoir capacity of each dispatch interval can be optimized considering not only the dispatch error observed at the corresponding time interval but also the error anticipated in upcoming intervals by controlling the power injection into ESS and adjusting the SoE at each time interval.

TABLE II
ESS ALLOCATION RESULT

Case	Location	Power rating	Energy reservoir
1	4	1.03MVA	1.99MWh
	27	521kVA	853kWh
2	4	915kVA	1.57MWh
	27	523kVA	773kWh

TABLE III
COST AND OPERATIONAL ADVANTAGE COMPARISON

Horizon		Case 0	Case 1	Case 2
10 yrs	Total cost ($Million)	9.48	1.54	1.74
	Investment cost ($Million)	-	1.36	1.19
	Penalty cost ($Million)	9.48	0.18	0.55
1 yr	Uncovered error (MWh)	1354.27	26.91	78.68
	Grid losses (MWh)	55.24	45.09	46.03
	Consumed energy (GWh)	7.357	7.488	7.419

The operational advantage of the ESS allocation and the superiority of case 1 over case 2 are well visualized in Fig. 4, which illustrates the operation simulation for typical day-type 1, showing the prosumption prediction based on 10 prosumption scenarios, the dispatch plan, and the active power flow through GCP (Node 1) for each scenario in the case of no ESS (see Fig. 4.(a)), and in the two cases of the optimal ESS allocation with and without the offset profile (see Fig. 4.(b) and Fig. 4.(c), respectively). Due to the prediction error of the prosumption forecast, the significant magnitude of power deviation from the scheduled power is observed, especially in the time when the PV power production is high. Therefore, without the support of ESS for compensating the dispatch error, the DSO is expected to pay a substantial amount of penalty cost. On the contrary, in the cases with the ESS allocated, the ESS effectively reduces the possible dispatch error, enforcing the active power flow through the GCP for each scenario to follow the dispatch plan. The difference in case 1 and case 2 is shown in the dispatch plan. In case 2, the dispatch plan is equivalent to the total prosumption profile considering grid losses. On the other hand, the dispatch plan in case 1 deviates from the total prosumption prediction profile, especially during the daytime because of the implementation of the offset profile. The offset profile takes value, particularly at the time intervals when the notable amount of dispatch error at the GCP is anticipated at the following time intervals successively. The power charge/discharge of the ESS corresponding to the offset profile can adjust the SoE level to have enough flexibility to cope with the imminent uncertainties. In this way, the uncovered dispatch error can be additionally reduced compared to the case 2.

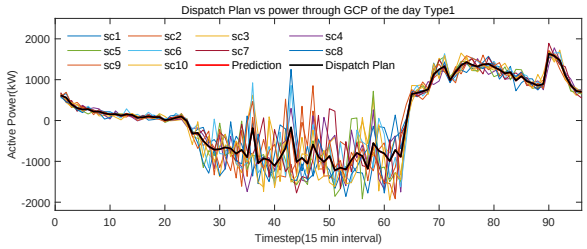

(a)

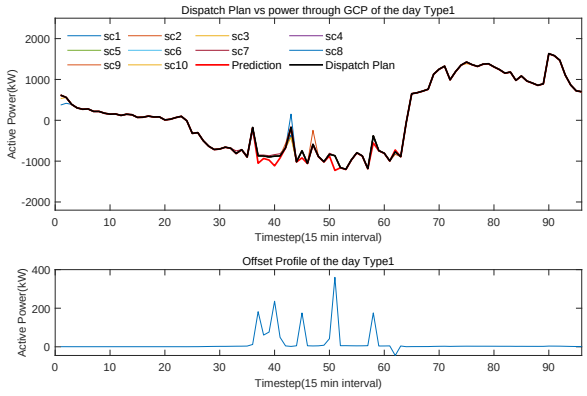

(b)

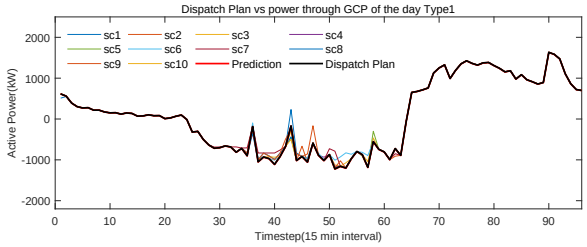

(c)

Fig. 4. Prosumption prediction, dispatch plan and active power through the GCP in each scenario (sc): (a) Case 0 (No ESS), (b) Case 1 (With ESS integrated with offset profile), (c) Case 2 (With ESS and without offset profile)

The effectiveness of the optimal ESS allocation accompanying the control scheme is assessed quantitatively by comparing the annual uncovered dispatch error in different cases. The difference in energy is then translated into a considerable gap in the total cost for 10 years of operation: $9.48 Million with the default system configuration, and $1.54 Million with the optimal ESS allocation integrating the offset profile. Consequently, the result shows the economic and technical excellence of investing in ESS for the interest of the DSO in attaining the controllability of the active power infeed through the GCP. Moreover, we successfully demonstrate that the implementation of the offset profile improves the potential of ESS to handle the uncertainties by maximizing its flexibility.

C. Comparison with the case of realistic imbalance price

The results of cases 1 and 2 are based on the adoption of an artificially high imbalance price to achieve the sufficient dispatchability of the ADN. It is worth to observe the change of the ESS allocation and resulting operational benefit when the imbalance penalty is set in a realistic market price. There-

fore, we add another simulation result (case 3), where all the conditions are identical to those of case 1 with the exception of the imbalance penalty replaced with a realistic imbalance price (i.e., \$43.5/MWh, obtained by averaging the imbalance prices in Swiss wholesale electricity market from 2013 to 2015 [26]). The optimal siting and sizing for case 3 are shown in Table IV, along with the corresponding cost and operation results. In comparison to case 1 (see Table II and Table III), we can observe a significant difference in ESS size that, however, results in \$1 Million difference in investment costs and 356.15 MWh difference in uncovered dispatch errors.

TABLE IV
ESS ALLOCATION AND COST RESULTS FOR CASE 3

ESS allocation	Node	Power rating	Energy reservoir
	4	598kVA	473kWh
Cost result	10 yrs	Total cost (\$Million)	0.53
		Investment cost (\$Million)	0.36
		Penalty cost (\$Million)	0.17
Operational result	1 yr	Unserved error (MWh)	383.06
		Grid losses (MWh)	48.06
		Consumed energy (GWh)	7.317

V. CONCLUSION

In this paper, we have proposed an effective tool for the optimal allocation of ESSs within an ADN to achieve its dispatchability. The specialty of the proposed method is the integration of an ESS control scheme so-called offset profile into a dispatch plan. The offset profile quantifies the necessary power injection to the ESS to optimize the exploitation of energy reservoir capacity of ESS. The operational benefit of ESSs with the control strategy embedded is evaluated through the daily operation of ADN, which is modeled by the linear approximated convex OPF, or the PWL-OPF model. This model is advantageous for guaranteeing the approximated global optimal solution while accounting for the operational conditions of the network with sufficient accuracy and small approximation error. Then, Benders decomposition is applied to handle the computational complexity of the planning problem. The effectiveness of the proposed method is validated through simulations conducted on the real Swiss ADN comprising 55 nodes and a large capacity of distributed renewable generation. The result underpins that the ESS allocation eliminates the dispatch error, and the dispatchability can be further enhanced with the integration of the ESS control scheme compared to the ESS planning approach without the contol scheme.

REFERENCES

[1] M. Bozorg, F. Sossan, J.-Y. Le Boudec, and M. Paolone, "Influencing the bulk power system reserve by dispatching power distribution networks using local energy storage," *Electr. Pow. Syst. Res.*, vol. 163, pp. 270–279, 2018.

[2] H. Holttinen, A. Tuohy, M. Milligan, E. Lannoye, V. Silva, S. Müller, L. Sö *et al.*, "The flexibility workout: managing variable resources and assessing the need for power system modification," *IEEE Power Energy Mag.*, vol. 11, no. 6, pp. 53–62, 2013.

[3] G. Koeppel and M. Korpås, "Improving the network infeed accuracy of non-dispatchable generators with energy storage devices," *Electr. Pow. Syst. Res.*, vol. 78, no. 12, pp. 2024–2036, 2008.

[4] T. Boutsika and S. Santoso, "Sizing an energy storage system to minimize wind power imbalances from the hourly average," in *2012 IEEE Power Energy Soc. General Meeting*. IEEE, 2012, pp. 1–8.

[5] R. R. Appino, J. Á. G. Ordiano, R. Mikut, T. Faulwasser, and V. Hagenmeyer, "On the use of probabilistic forecasts in scheduling of renewable energy sources coupled to storages," *Applied energy*, vol. 210, pp. 1207–1218, 2018.

[6] F. Sossan, E. Namor, R. Cherkaoui, and M. Paolone, "Achieving the dispatchability of distribution feeders through prosumers data driven forecasting and model predictive control of electrochemical storage," *IEEE Trans. Sustain. Energy*, vol. 7, no. 4, pp. 1762–1777, Oct 2016.

[7] J. P. Chaves-Ávila, R. A. Hakvoort, and A. Ramos, "The impact of european balancing rules on wind power economics and on short-term bidding strategies," *Energy Policy*, vol. 68, pp. 383–393, 2014.

[8] E. Stai, L. Reyes-Chamorro, F. Sossan, J. Le Boudec, and M. Paolone, "Dispatching stochastic heterogeneous resources accounting for grid and battery losses," *IEEE Trans. Smart Grid*, vol. 9, no. 6, pp. 6522–6539, Nov 2018.

[9] P. Fortenbacher, A. Ulbig, and G. Andersson, "Optimal placement and sizing of distributed battery storage in low voltage grids using receding horizon control strategies," *IEEE Transactions on Power Systems*, vol. 33, no. 3, pp. 2383–2394, 2018.

[10] P. Pinson *et al.*, "Dynamic sizing of energy storage for hedging wind power forecast uncertainty," in *2009 IEEE Power Energy Soc. General Meeting*. IEEE, 2009, pp. 1–8.

[11] H. Bludszuweit and J. A. Domínguez-Navarro, "A probabilistic method for energy storage sizing based on wind power forecast uncertainty," *IEEE Trans. Power Syst.*, vol. 26, no. 3, pp. 1651–1658, 2010.

[12] J. H. Yi, R. Cherkaoui, and M. Paolone, "Optimal siting and sizing of energy storage systems in active distribution networks to achieve their dispatchability," *arXiv preprint arXiv:1909.12667*, 2019.

[13] X. Ke, N. Lu, and C. Jin, "Control and size energy storage systems for managing energy imbalance of variable generation resources," *IEEE Trans. Sustain. Energy*, vol. 6, no. 1, pp. 70–78, 2014.

[14] A. Giannitrapani *et al.*, "Optimal allocation of energy storage systems for voltage control in lv distribution networks," *IEEE Trans. Smart Grid*, vol. 8, no. 6, pp. 2859–2870, 2016.

[15] S. H. Low, "Convex relaxation of optimal power flowpart i: Formulations and equivalence," *IEEE Trans. Control Netw. Syst.*, vol. 1, no. 1, pp. 15–27, 2014.

[16] Q. Li, R. Ayyanar, and V. Vittal, "Convex optimization for des planning and operation in radial distribution systems with high penetration of photovoltaic resources," *IEEE Trans. on Sustain. Energy*, vol. 7, no. 3, pp. 985–995, 2016.

[17] E. Grover-Silva *et al.*, "Optimal sizing and placement of distribution grid connected battery systems through an socp optimal power flow algorithm," *Applied Energy*, vol. 219, pp. 385–393, 2018.

[18] M. Nick, R. Cherkaoui, J. L. Boudec, and M. Paolone, "An exact convex formulation of the optimal power flow in radial distribution networks including transverse components," *IEEE Trans. Autom. Control*, vol. 63, no. 3, pp. 682–697, March 2018.

[19] R. Gupta, F. Sossan, and M. Paolone, "Performance assessment of linearized opf-based distributed real-time predictive control," in *2019 IEEE Milan PowerTech*, June 2019, pp. 1–6.

[20] R. A. Jabr, "High order approximate power flow solutions and circular arithmetic applications," *IEEE Trans. Power Syst.*, pp. 1–1, 2019.

[21] J. F. Franco, M. J. Rider, M. Lavorato, and R. Romero, "Optimal conductor size selection and reconductoring in radial distribution systems using a mixed-integer lp approach," *IEEE Trans. Power Syst.*, vol. 28, no. 1, pp. 10–20, Feb 2013.

[22] M. Shafie-Khah, P. Siano, D. Z. Fitiwi, N. Mahmoudi, and J. P. S. Catalo, "An innovative two-level model for electric vehicle parking lots in distribution systems with renewable energy," *IEEE Trans. Smart Grid*, vol. 9, no. 2, pp. 1506–1520, March 2018.

[23] P. L. Cavalcante, J. C. Lpez, J. F. Franco, M. J. Rider, A. V. Garcia, M. R. R. Malveira, L. L. Martins, and L. C. M. Direito, "Centralized self-healing scheme for electrical distribution systems," *IEEE Trans. Smart Grid*, vol. 7, no. 1, pp. 145–155, Jan 2016.

[24] A. M. Geoffrion, "Generalized benders decomposition," *J. Optimiz. Theory App.*, vol. 10, no. 4, pp. 237–260, 1972.

[25] A. K. Jain, R. C. Dubes *et al.*, *Algorithms for clustering data*. Prentice hall Englewood Cliffs, NJ, 1988, vol. 6.

[26] J. Abrell, "The swiss wholesale electricity market," *tech. rep., wiss Competence Center for Energy Research*, 2016.